Pergamon

Int. J. Heat Mass Transfer. Vol. 40, No. 6, pp. 1491–1500, 1997

0017–9310/97 $17.00+0.00

PII: S0017–9310(96)00070–1

Impingement heat transfer and recovery effect with submerged jets of large Prandtl number liquid—II. Initially laminar confined slot jets

C. F. MA, Y. ZHUANG and S. C. LEE
Beijing Polytechnic University, Beijing 100022, People's Republic of China

and

T. GOMI
Sophia University, Tokyo 102, Japan

(*Received for publication* 7 *March* 1996)

Abstract—Local measurements were made to determine recovery factors and heat transfer coefficients resulting from the impingement of transformer oil jets issuing from tiny slot nozzles of 0.091, 0.146, and 0.234 mm in width. This study focused on initially laminar jets in the range of jet Reynolds number between 55 and 415, and fluid Prandtl number between 200 and 270. Lateral distribution of local recovery factor was measured at various Reynolds numbers and nozzle-to-plate distances. Stagnation point heat transfer coefficient was collected and correlated as a function of jet Reynolds number, nozzle-to-plate spacing and nozzle width. Twenty seven lateral profiles of local heat transfer were obtained and correlated. Non-monotonic variation and unusual behavior of local heat transfer were observed and attributed to possible transition from laminar to turbulent regime. Based on the measured local data, integral average heat transfer rate was determined and correlated. Copyright © 1996 Elsevier Science Ltd.

1. INTRODUCTION

Experimental investigations of heat transfer under planar liquid jets have been reviewed by Webb and Ma [1]. In the previous investigations water was most extensively employed as the working fluid [2–10]. Only two studies were performed with test liquid other than water: PAO by Gu *et al.* [11] and FC-72 by Wadsworth and Mudawar [12]. These investigations have focused largely on jet Reynolds number ranges for which the impinging jet flow at the nozzle exit was fully turbulent. Only four reports [2, 10–12] were related to impinging jets at initially laminar regime. It is also noted that all the experimental studies [2–9, 11] in the open literature conducted with free-surface planar liquid jets, except for the work in Purdue [10, 12] aimed at micro-electronic cooling. However, both the two reports concerning submerged planar jets are related to average heat transfer. The lack of information on submerged planar liquid jets may be partially compensated by using the experimental results of planar air jets, which are available more extensively in open literature [13]. Nevertheless, as the Prandtl number of liquid may be one or several orders of magnitude higher than that of gas, the extrapolation of air jet knowledge to the cases of liquid jets should be reviewed with caution on this basis alone. The key issue is the dependence of impingement heat transfer on Prandtl number. At present, the Prandtl number dependence has not been examined for planar jets. Moreover, for large Prandtl number liquid, the recovery effect may be an important factor in the impingement heat transfer process. But it has not been reported with planar jets yet. The purpose of this work is to fill these gaps in heat transfer data base. Three nozzles of small width ($B = 0.091$, 0.146 and 0.234 mm) were employed in the experiments with transform oil as the test liquid ($Pr = 200$–270). The local heat transfer characteristics of submerged planar jets were investigated in the range of jet Reynolds number between 55 and 415, in which no previous study has explored and characterized the thermal process with submerged slot liquid jets.

2. EXPERIMENTAL APPARATUS AND PROCEDURE

The experimental apparatus and procedure have been described in the part 1 of this work. Here we only provide the description of the jet nozzle assembly in detail.

Three slot nozzles were constructed and employed in the present study. All the nozzles were made of Plexiglas. Figure 1 shows the configuration of the jet nozzles. The three rectangular ducts have the same streamwise length of 35 mm, and different dimensions of the cross-sections: 0.091, 0.146, and 0.234 mm in

NOMENCLATURE

$a, \bar{a}$	empirical constants
$b, \bar{b}$	empirical constants
B	slot width
$c, \bar{c}$	empirical constants
C_p	specific heat
$d, \bar{d}$	empirical constants
$e, \bar{e}$	empirical constants
G	velocity gradient
h	local heat transfer coefficient
H	length of target plate
k	thermal conductivity of the fluid
K	empirical constants
L	potential core length
m, n	empirical constants
$\underline{Nu}$	local Nusselt number $Nu = h \cdot 2B/k$
$\overline{Nu}$	local average Nusselt number
p, q	empirical constants
r	recovery factor
Re	Reynolds number, $Re = u \cdot X/v$
T_{aw}	adiabatic wall temperature
T_j	jet static temperature at nozzle exit
T_w	wall temperature
u	mean fluid velocity at nozzle exit
v	mean axial velocity component
v'	rms fluctuation in v
X	coordinate along the impingement surface with origin at the stagnation point
Z	nozzle-to-plate spacing
ν	kinematic viscosity.

Subscripts

0	stagnation point
max	maximum
c	critical.

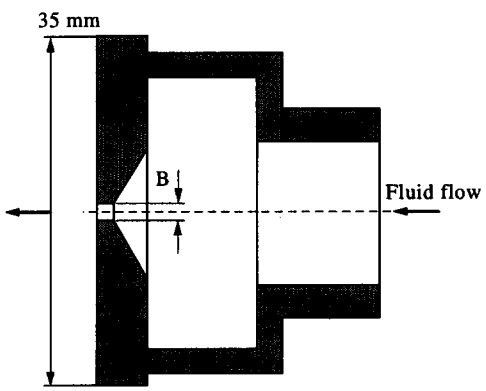

Fig. 1. Jet nozzle assembly.

width, respectively and 12 mm in height. The large aspect ratio between height and width eliminates the end effect and leads to a situation of truly two dimensional jets. Great efforts were made to control the parallelism of the two larger walls of the rectangular tubes. The shape and size of the nozzles were precisely measured with the tool maker's microscope of 0.001 mm resolution. The nozzles, particularly the smaller ones of 0.091 and 0.146 mm in width, were reconstructed several times until good quality was obtained. According to the correlation recommended in ref. [14], fully developed laminar profiles of mean velocity were obtained for the three nozzles in the entire range of the present study.

3. EXPERIMENTAL RESULTS AND DISCUSSION

3.1 *Recovery factor*

Lateral variation of the wall temperature on the target plate was measured when the surface heat flux was zero with the three nozzles at a constant jet velocity of 15 m s^{-1} in the range of nozzle-to-plate spacing between 2 and 32. This measurement provided the adiabatic wall temperature. Then, the following equation was used to calculate recovery factor:

$$r = \frac{T_{aw} - T_j}{u^2/2C_p}. \quad (1)$$

Eight profiles of the local recovery are presented in Fig. 2. Inspection of these graphs indicates that all the profiles are similar with each other. A minimum appears at the stagnation point. A pair of maxima, symmetrical to stagnation line, are recorded around $X/B \approx \pm 3$. Beyond the maxima, the recovery factor declines gradually with lateral distance from stagnation point. The two profiles in Fig. 2(a) exhibit the significant effect of nozzle-to-plate spacing on recovery factor. It is observed from the figure that the recovery factor for $Z/B = 20$ is almost 90% higher than that for $Z/B = 32$. But this effect seems insignificant with smaller Z/B. The experimental data presented in Fig. 2(b) display slight influence of spacing, as well as the jet velocity, on the recovery factor. If comparison is made between the present result and the experimental data of submerged circular jets reported in Part I of this work, it can be observed that the maxima of the former are much lower than those of the latter. It is also noted that the variation of recovery factor of planar jets with the lateral distance is much less pronounced than that of circular jets. As information of planar jet recovery factor is not available in literature, it is impossible to make comparison of the present data with any result from other resources. However, a numerical study has been conducted by the present authors to explore the recovery

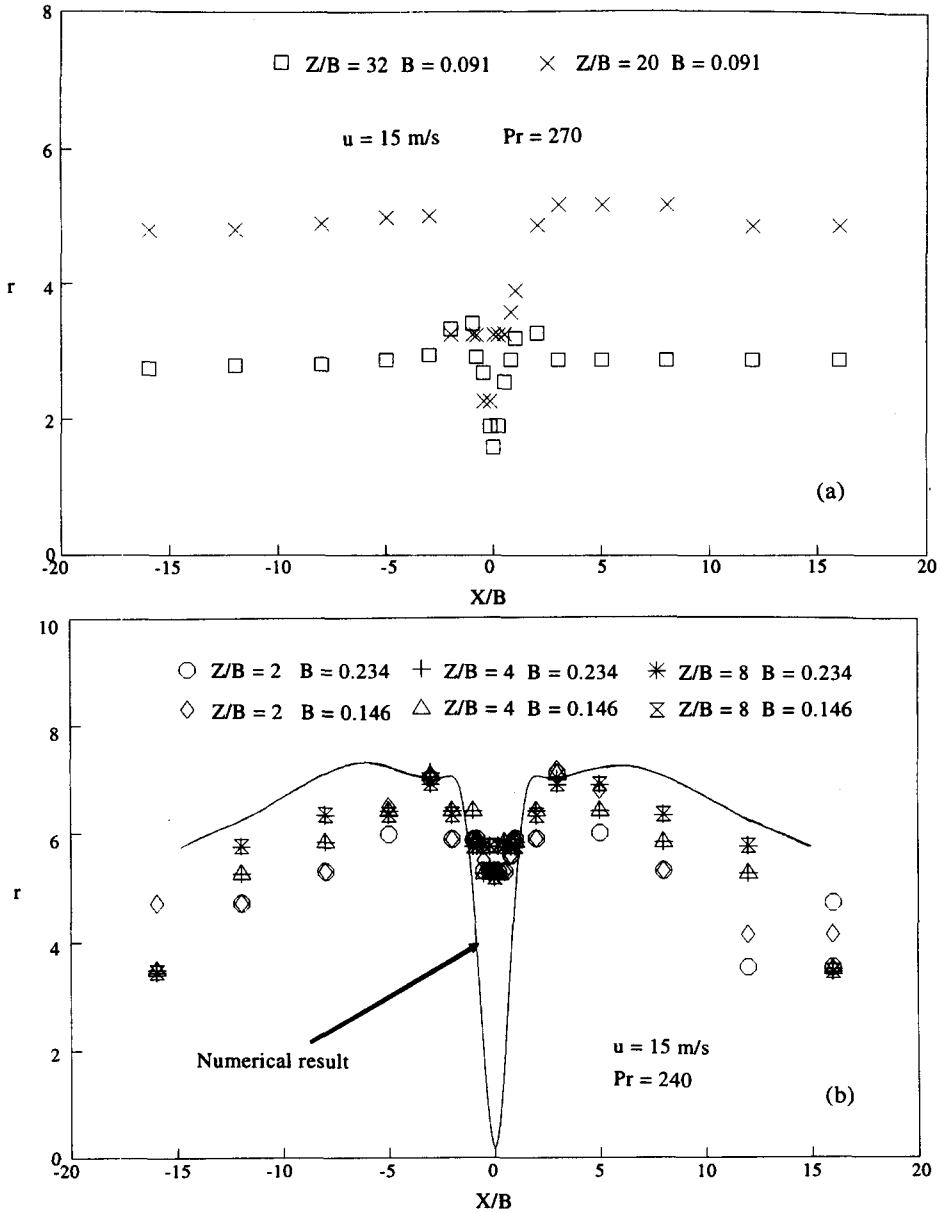

Fig. 2. Lateral distribution of the recovery factor: (a) $B = 0.091$ mm; (b) $B = 0.146$ and 0.234 mm.

effect of submerged slot jets. A numerical profile of recovery factor for 0.234 mm nozzle at $u = 15$ m s^{-1} and $Z/B = 4$ is presented in Fig. 2(b) for comparison. A general agreement is seen between the numerical result and the experimental data.

3.2. *Heat transfer at stagnation point*

Stagnation point heat transfer rates were measured and collected as a function of nozzle size, nozzle exit velocity and nozzle-to-plate spacing. The results are exhibited in Figs. 3–5. Figure 3 illustrates the variation of stagnation point Nusselt number with jet Reynolds number for the three nozzle sizes at $Z/B = 4$ and 8, respectively. As shown in the figure, there is a distinct nozzle size dependence in the functional relationship of stagnation point Nusselt number with jet Reynolds

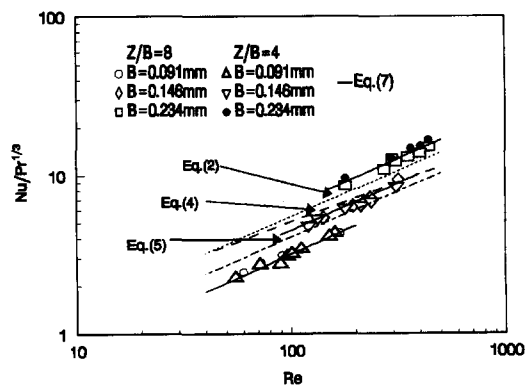

Fig. 3. Stagnation point heat transfer with different nozzle widths.

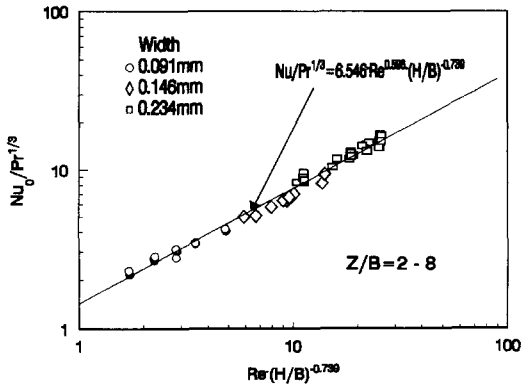

Fig. 4. Correlation of stagnation point heat transfer.

number. Higher stagnation point transfer rates were observed for larger nozzles. The data with nozzle of 0.234 mm and 0.146 mm width are about 100 and 40% higher than those with 0.091 mm nozzle at $Z/B = 4$, respectively. This observation is consistent with the results of planar air jets [15]. This trend was also reported for circular submerged water jets by Elison and Webb [16] with the nozzle diameter from 0.25 mm to 0.5 mm in the range of $Re = 300$–7000. The size dependence was ascribed to reduction of the initial turbulence for initially turbulent jets by Gardon and Akfirat [15]. They found that the turbulence intensity declined from 7.5 to 0.6% with decreasing nozzle width from 1/4 to 1/16 in at $Re = 1.1 \times 10^4$. It might be expected that this effect of initial turbulence would

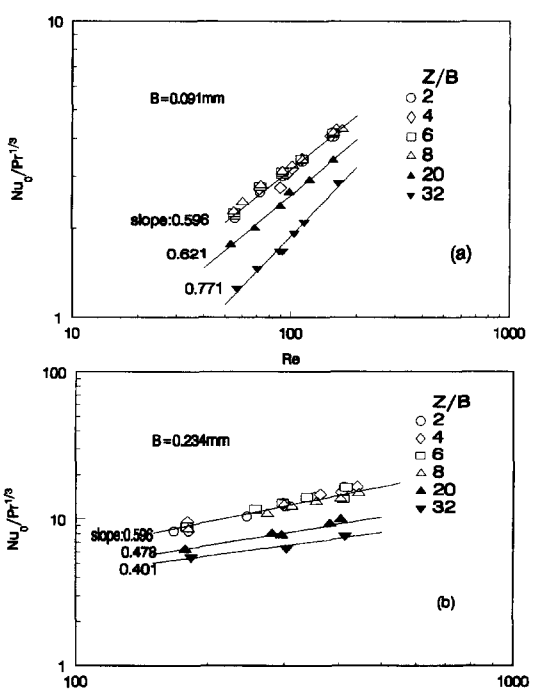

Fig. 5. Variation of stagnation point Nusselt number with jet Reynolds number at various nozzle-to-plate spacings: (a) $B = 0.091$ mm; (b) $B = 0.234$ mm.

be more pronounced for initially laminar liquid jets in the present study. However, to the best knowledge of the present authors, there is no information of turbulence intensity for planar jets in the initially laminar regime. Further research is required for the explanation of this trend, particularly for tiny liquid jets.

Stagnation point heat transfer data are not available with submerged planar liquid jet in open literature. In Beijing Polytechnic University, local heat transfer has been measured and correlated with FC-72 submerged slot jets of 0.21 mm in width [17]. The following correlation was recommended for stagnation line:

$$Nu_0 = 0.383 Re^{0.577} Pr^{1/3}. \quad (2)$$

As shown in Fig. 3, the agreement of equation (2) with the present data of $B = 0.234$ mm is quite good. The present results concerning stagnation point heat transfer are also compared with the correlations developed for free surface planar water jets. It was testified in this work that the difference in heat transfer at stagnation point between submerged and unsubmerged jet was less than 4%. Based on previous studies, a stagnation Nusselt number expression was recommended for planar laminar jets with $Pr = 0.7$–10 by Vader *et al.* [5]:

$$Nu_0 = 0.505 Re^{0.5} Pr^{0.376}. \quad (3)$$

This correlation has been verified with the experimental data reported by Inada *et al.* [2] at $Re = 940$ for low-turbulence water jet with near-uniform velocity profiles. For large Prandtl number liquid, equation (3) may be modified by altering the exponent of Pr number slightly from 0.376 to 1/3:

$$Nu_0 = 0.505 Re^{0.5} Pr^{1/3} \quad (4)$$

where the power 1/3 was recommended to transformer oil jet by Ma *et al.* [9].

Predicted curve by equation (4) is presented in Fig. 3. The curve lies between the data for the widths of 0.146 mm and 0.234 mm, indicating the general agreement between the present results and the analytical correlation. The experimental data are also compared with the empirical correlation presented for water jets of 10 mm width at $Re = 2 \times 10^4$–9×10^4 by Vader *et al.* [5] after the same modification concerning Prandtl number dependence:

$$Nu_0 = 0.28 Re^{0.58} Pr^{1/3}. \quad (5)$$

General agreement is observed between the present data and the equation (5) as shown in Fig. 3. Considering the significant differences in fluid Prandtl number, Reynolds number and nozzle geometry between the investigations, the discrepancy between equations (2),(4) and (5) and the present data should not be beyond expectation.

It was verified for free-surface planar water jets that stagnation flow heat transfer can be expressed by four independent variables [7]

$$Nu_0 = 0.849 Re^{0.584} G^{0.36} (\overline{v'/v})^{0.263} Pr^{0.4}. \quad (6)$$

The two terms G and $(\overline{v'/v})$ are included in the correlation attempting to describe the effects of velocity gradient and turbulence intensity on the heat transfer, respectively. For the tiny jets investigated in this work, it seems impossible to make measurements for the two items. Equation (6) may be modified by displacement of the two items with dimensionless nozzle width B/H to characterize the effect of nozzle width on the flow and heat transfer at stagnation zone:

$$Nu_0 = K Re^m Pr^n (H/B)^p \quad (7)$$

where the Prandtl number power $n = 1/3$ was adopted for large Pr number liquid jets from refs. [17, 19]. The coefficient K and exponents m and p were obtained by a least-squares technique using all the data of the three nozzles within $Z/B \leqslant 8$. The values were determined to be $K = 6.546$, $m = 0.596$ and $p = -0.739$. The correlation is within $\pm 10\%$ of 93% of the experimental data, with an average error of $\pm 4.1\%$ and a standard deviation of 5.3% as shown in Fig. 4. It is noted that the Reynolds number power 0.596 is almost identical with the values of 0.577 for submerged FC-72 slot jets [17], 0.58 for free-surface planar water jets [5], 0.6 for planar air jets [18], and close to 0.608 and 0.71 reported for free-surface planar water jets by Zumbrunnen *et al.* [9] and Wolf *et al.* [7], respectively.

The comparison of equation (7) with the experimental data at different constant nozzle-to-plate spacings is presented in Fig. 5. Good agreement is observed both for the two nozzles with the data for $Z/B \leqslant 8$. Beyond this distance, the increase of nozzle-to-plate spacing likely results in change in the slope of $Nu_0 Pr^{-1/3} \sim Re$ curves. As illustrated in Fig. 5, increase in the slope from 0.596 to 0.621 and 0.771 and decrease from 0.596 to 0.478 and 0.401 are recorded with 0.091 mm and 0.234 mm nozzles, respectively. The reason for the difference is not clear at present.

The effect of nozzle-to-plate spacing on the stagnation point heat transfer is examined in greater detail in Fig. 6, where the Nu_0 is plotted as a function of the dimensionless separation distance Z/B for different nozzles in the range of $Re = 55$–407. It is seen from the figures that the variation of Nu_0 with Z/B, which may not be monotonic, exhibits a complex nature depending on Reynolds number and nozzle geometry. Within a certain dimensionless length of the spacing L/B, the Nusselt number is essentially independent on the separation distance. The values of L/B seem to increase with decreasing of the nozzle width, and are approximately determined from the experimental data to be 7, 10 and 12 for the nozzle widths 0.234, 0.146 and 0.091 mm, respectively. Beyond these dimensionless spacing lengths, a general diminution of the heat transfer coefficient is apparently observed with increasing separation distance. This trend is consistent with the results reported for planar air jets [15, 18] and circular water jets [16, 20]. Inspection of the data

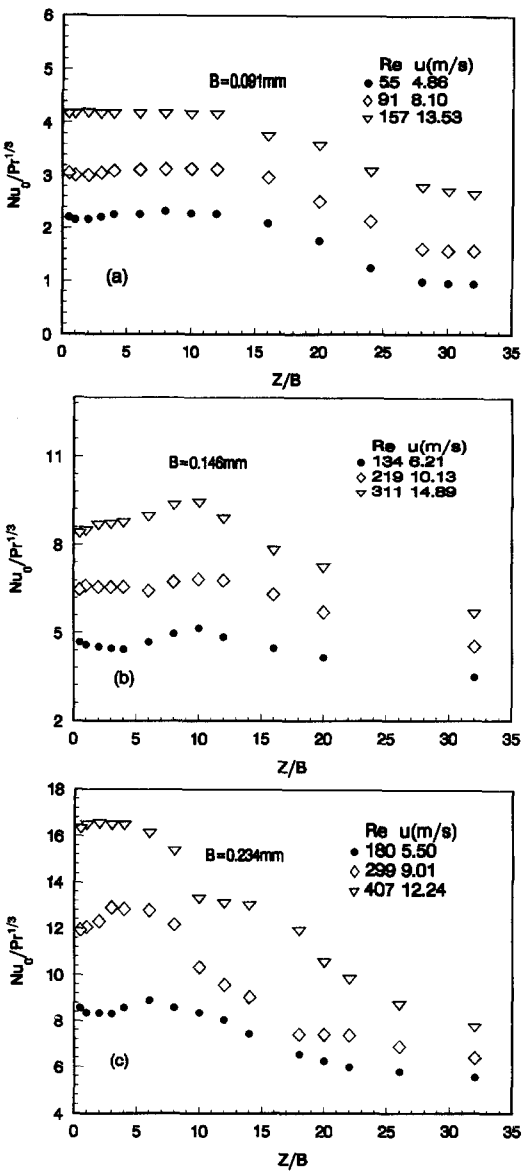

Fig. 6. Variation of stagnation Nusselt number with nozzle-to-plate spacing for the three nozzle widths: (a) $B = 0.091$ mm; (b) $B = 0.146$ mm; (c) $B = 0.234$ mm.

in Fig. 6(c) reveals non-monotonic variation of Nu_0 with Z/B at $Re = 407$ and 299 for the nozzle of 0.234 mm width. These experimental data were reproduced several times to ensure the repeatability in this work. Similar non-monotonic behavior was also observed with planar air jets by Gardon and Akfirat [15] and Sparrow and Wong [18] both at the same higher Reynolds numbers (950 and 650).

It has been found for planar air jets [15, 18, 21] that the variation of stagnation point heat transfer with separate distance is affected by two factors: arrival jet velocity at the centerline and the turbulence intensity. When leaving the nozzle immediately, the jet begins to entrain the surrounding quiescent fluid. The width of the mixing regime increases continuously. At some

distance from the nozzle exit the mixing zone penetrates to the centerline of the jet. The corresponding length of the separate distance is so-called potential core length (L). Within the potential core, the jet velocity at centerline remains unchanged, being independent of the separation distance and the heat transfer coefficient should exhibit a corresponding trend. Beyond the potential core, the centerline jet velocity decreases with $Z^{-1/2}$ [21], resulting diminution of the heat transfer at stagnation point. As to turbulence, it was reported in ref. [21] that the turbulence generated by mixing of planar air jets increases with the nozzle-to-plate spacing until reaching a maximum as high as an order of 30% in the neighborhood of $Z/B = 8$, then declines progressively. The turbulence significantly enhances the impingement heat transfer. The variation of stagnation point heat transfer with separate distance is mainly governed by the two conflicting factors. Based on the above discussion, an attempt was made to develop correlations for the experimental data collected in this work beyond the potential core. The correlations are of the following form:

$$Nu_0/Nu_{0,\max} = \left(\frac{L/B}{Z/B}\right)^q \tag{8}$$

where the empirical constant q was obtained from experimental data with L/B being set equal to the values mentioned in foregoing section. The values of the constants and the errors of the correlations are given in Table 1.

Comparison of equation (8) with the experimental data normalized to the maximum Nusselt number is presented in Fig. 7. The data and the curves clearly indicate the presence of the potential core, the general decline of the stagnation point Nusselt number beyond the potential core, and the slight increase of Nu_0 with the spacing inside the potential core in several cases resulted from the turbulence enhancement. For lack of information concerning the flow characteristics with tiny jets of large Prandtl number liquid, it seems difficult to provide explanation for the non-monotonic behavior observed in this work.

Table 1. Constants and errors in equation (8)

Nozzle width [mm]	0.091	0.146	0.234
L/B	12	10	7
q	0.584	0.329	0.433
Average error	±7.2%	±3.7%	±7.5%
Standard deviation	10.4%	5.9%	9.0%
Maximum deviation	23.5%	7.2%	16.6%

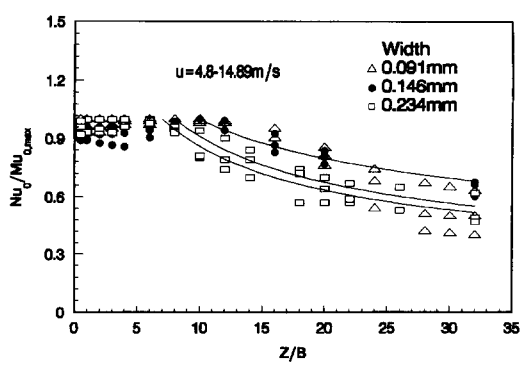

Fig. 7. Correlation of stagnation Nusselt number with nozzle-to-plate spacing at constant Reynolds numbers.

3.3. *Lateral variation of local heat transfer*

Lateral distribution of local heat transfer was measured with the three nozzles. The effect of jet velocity and nozzle-to-plate spacing was examined in experimental detail. At total, 27 profiles were obtained in the range of $Re = 67$–414 and $Z/B = 2$–32. The experimental data are plotted in Fig. 8 after normalization to the heat transfer coefficient at stagnation point where the maximum occurs.

As shown in the figures, all the profiles are generally of bell shape with a peak appearing at stagnation point. The heat transfer coefficients, excluding those at $X/B > 5$ in Figs. 8(c)–(e), decrease monotonically with increasing the lateral distance from stagnation point. This trend is apparently resulted from the thickening of the wall jet flow along the target surface.

In order to examine the local variation of heat transfer coefficient in more detail, some profiles are represented in Fig. 9 without normalization. As illustrated in Fig. 9, humps of the heat transfer distribution curves are clearly observed with all the 12 profiles at different Reynolds numbers. For six profiles, both a local minimum and a maximum are recorded with a same curve. The local Nusselt number declines from the stagnation point until the local minimum appears, then increases with increasing of lateral distance reaching a second peak. Beyond this peak the local heat transfer coefficient decreases again. Similar heat transfer phenomenon was reported with planar air jets by Sparrow and Wong [18], and attributed to the free stream turbulence generated by the mixing of the impingement flow with the quiescent environment or the possible transition from laminar to turbulent regime. It may be noted in this work that although the flow Reynolds number is low ($Re < 414$), the absolute flow velocity between 4.86 and 13.53 m s^{-1} is much higher than those in many previous studies with planar liquid jets [5, 7, 9]. The minimum and maximum might be the symptoms of the onset and completion, respectively, of the possible transition. For the other six profiles shown in the figures, only the minimum is observed. Probably, the heaters were too short at these conditions for complete development of the turbulent boundary layer. The incipience of the turbulent boundary layer may be estimated by the local Reynolds number based on the lateral distance from the stagnation point to the location corresponding to minimum heat transfer coefficient:

$$Re_{x,c} = \frac{u^* x}{v}. \tag{9}$$

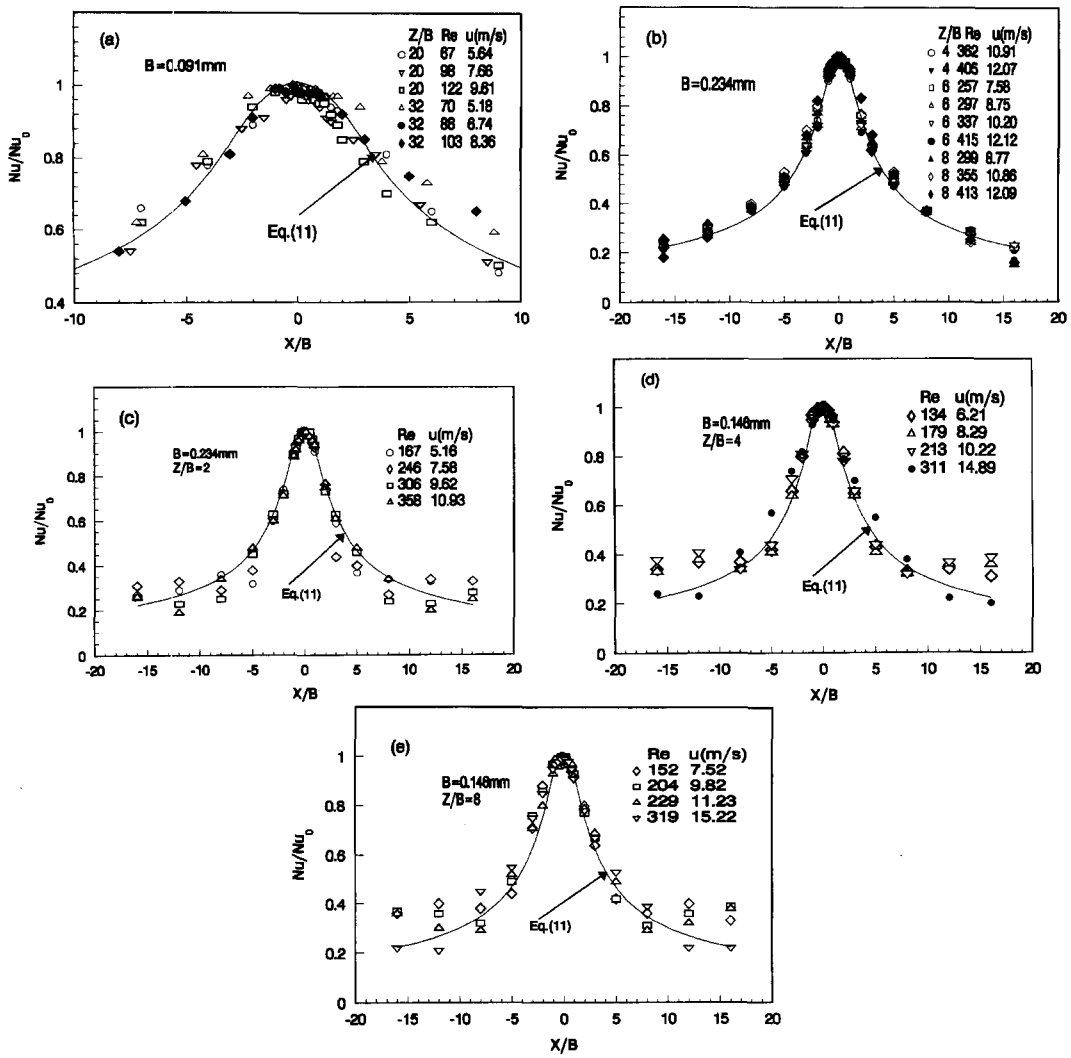

Fig. 8. Lateral profiles of the normalized local Nusselt number: (a) $B = 0.091$ mm; (b) $B = 0.234$ mm ($Z/B = 4$–8); (c) $B = 0.234$ mm ($Z/B = 2$); (d) $B = 0.146$ mm ($Z/B = 4$); (e) $B = 0.146$ mm($Z/B = 8$).

The data of $Re_{x,c}$ collected in this work are plotted as a function of jet Reynolds number in Fig. 10. These data of $Re_{x,c}$ can be well correlated by an empirical formula:

$$Re_{x,c} = 0.482Re^{1.54}. \quad (10)$$

Presented in Fig. 10 are also the data quoted from ref [18] for comparison. The trend exhibited by the critical Reynolds number $Re_{x,c}$ from the present work is generally consistent with that reported by Sparrow and Wong. But the present data are higher than those by Sparrow and Wong. The discrepancy is certainly resulted from the big difference in working fluid and nozzle geometry between the two investigations. Both the two results pertaining to $Re_{x,c}$ are much lower than the critical Reynolds number of 1.9×10^5 [9], 3.6×10^6 [3, 5] and $(1.5$–$4.6) \times 10^6$ [8] reported for free-surface planar water jets of 10 mm width. It is seen from the figure that the value of $Re_{x,c}$ significantly increases with increasing the jet Reynolds number. This phenomenon is also observed from Fig. 9. The local minimum appears at smaller lateral distance with decreasing the jet velocity. This anomalous variation is entirely different with the results reported for planar water jets [3, 5, 9]. The accelerating transition might be presumably due to the destabilization of laminar wall jet flow, which likely intends to occur at lower Reynolds number. For lack of any information of experimental result pertaining to the flow characteristics associated with submerged slot liquid jets issuing from tiny nozzles, it seems very difficult, if not impossible, to provide a convincing argumentation to explain this heat transfer behavior.

Another anomaly observed in this work is the non-monotonic variation of local heat transfer with Reynolds number. The dependence of Nusselt number on Reynolds number was examined for the profiles plotted in Fig. 9 at $X/B = 5$, 12 and 16. The experimental data are represented in Fig. 11. Before the onset of the transition ($X/B = 5$), the two curves exhi-

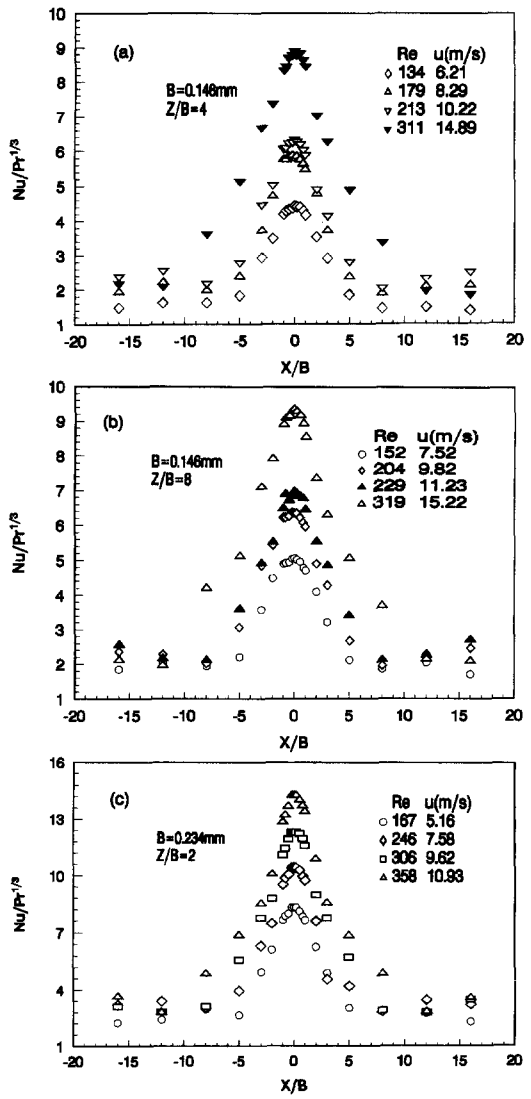

Fig. 9. Lateral variation of local heat transfer coefficient: (a) $B = 0.146$ mm $Z/B = 4$; (b) $B = 0.146$ mm $Z/B = 8$; (c) $B = 0.234$ mm $Z/B = 2$.

bit normal Reynolds number dependence: Nusselt number is approximately proportional to the square root of Reynolds number as shown in the figure. After the transition, anomalous variations of Nusselt number were recorded at $X/B = 12$ and 16 where higher Reynolds numbers could yield lower Nusselt numbers. It is also noteworthy in Fig. 11 that heat transfer coefficient at larger lateral location $X/B = 16$ may be higher than those at smaller location $X/B = 12$. The non-monotonic trend of decline in Nusselt number with increasing Reynolds number and decreasing lateral distance may be ascribed to the variation of turbulence intensity associated with the laminar–turbulent transition. Stronger turbulence intensity might be induced by the accelerating transition at lower Reynolds numbers, and consequently reduced the impedance to local heat transfer, resulting in the anomalous heat transfer characteristics in the wall jet zone after the transition. Further research is still required to clarify the enhancement mechanism.

An attempt was made to develop an empirical formula for correlating the local heat transfer data, excluding those affected by the possible transition. The correlation can be expressed by:

$$\frac{Nu}{Nu_0} = \left\{\left[\frac{\tanh a(X/B)}{X/B}\right]^b + [c\cdot(X/B)^d]^e\right\}^{1/e} \quad \text{for } X/B > 0 \qquad (11)$$

where the coefficients a, b, c, d and e were determined by a least-square technique from the experimental data. The values of the coefficients and the correlation errors are given in Table 2.

The correlation curves are presented in Fig. 8. Good agreement is seen between the data unaffected by the transition and the correlation curves.

3.4. *Average heat transfer*

The local heat transfer distributions were numerically integrated over different areas of the plate to determine the variation of the average heat transfer coefficient. After integration, the non-monotonic variation associated with local heat transfer profiles in Fig. 9 was somewhat smoothed. In consequence, all the average heat transfer data, including those affected by laminar–turbulent transition can be correlated by a formula of the same form of equation (11)

$$\frac{\overline{Nu}}{Nu_0} = \left\{\left[\frac{\tanh \bar{a}(X/B)}{X/B}\right]^{\bar{b}} + \left[\bar{c}\cdot(X/B)^{\bar{d}}\right]^{\bar{e}}\right\}^{1/\bar{e}} \quad \text{for } X/B > 0 \qquad (12)$$

where the coefficients $\bar{a}$, $\bar{b}$, $\bar{c}$, $\bar{d}$, $\bar{e}$ were obtained from the integral results from experimental data. Table 3 presents the values of these coefficients and the errors of the correlation.

Table 2. Empirical constants in equation (11) and the correlation errors

Nozzle width [mm]	Z/B	a	b	c	d	e	Average error	Standard deviation	Data points percentage inside ± 10% range
0.091	20–32	1.189	0.468	1.49	−0.483	−9	±4.48%	6.36%	91.2%
0.146	2–8	1.189	6.681	1.327	−0.644	−17	±3.91%	5.26%	95.2%
0.234	2–8	1.189	6.681	1.327	−0.644	−17	±3.91%	5.26%	95.2%

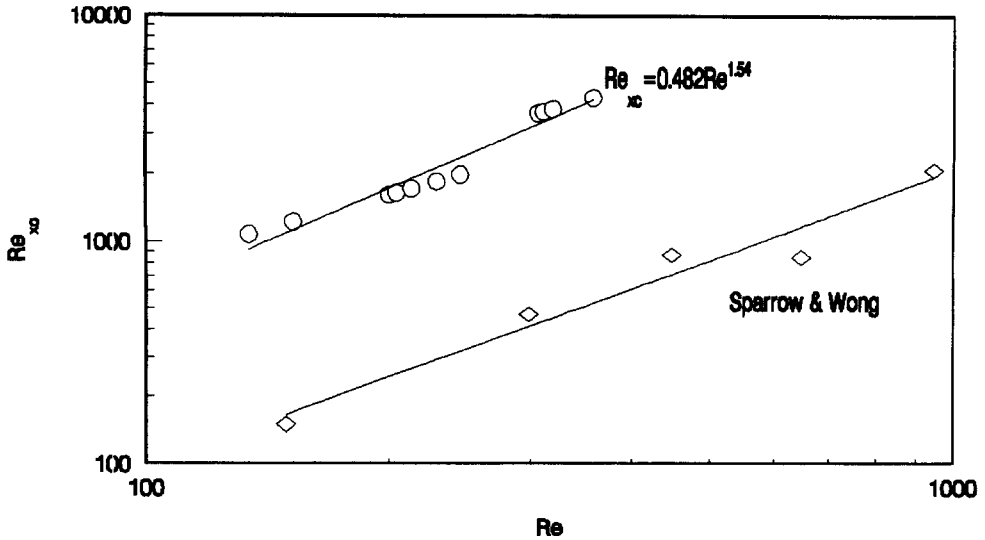

Fig. 10. Variation of critical Reynolds number $Re_{x,c}$.

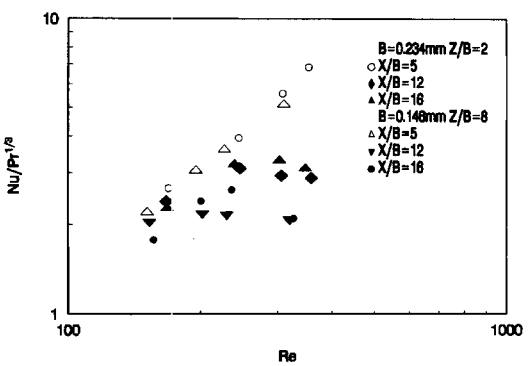

Fig. 11. Normal and anomalous variation of Nusselt number with jet Reynolds number at various lateral locations.

A comparison of the correlation and the integral results obtained from the experimental data is provided in Fig. 12, where the vertical bars present the ranges of the data scatter. If comparison is made between Figs. 12 and 8 or Tables 2 and 3, it will be found that the agreement between average heat transfer results, including the data affected by the transition, and equation (12) is better than that between local data and equation (11).

4. CONCLUSIONS

(1) Experimental study was performed to investigate heat transfer and recovery effect with impinging slot

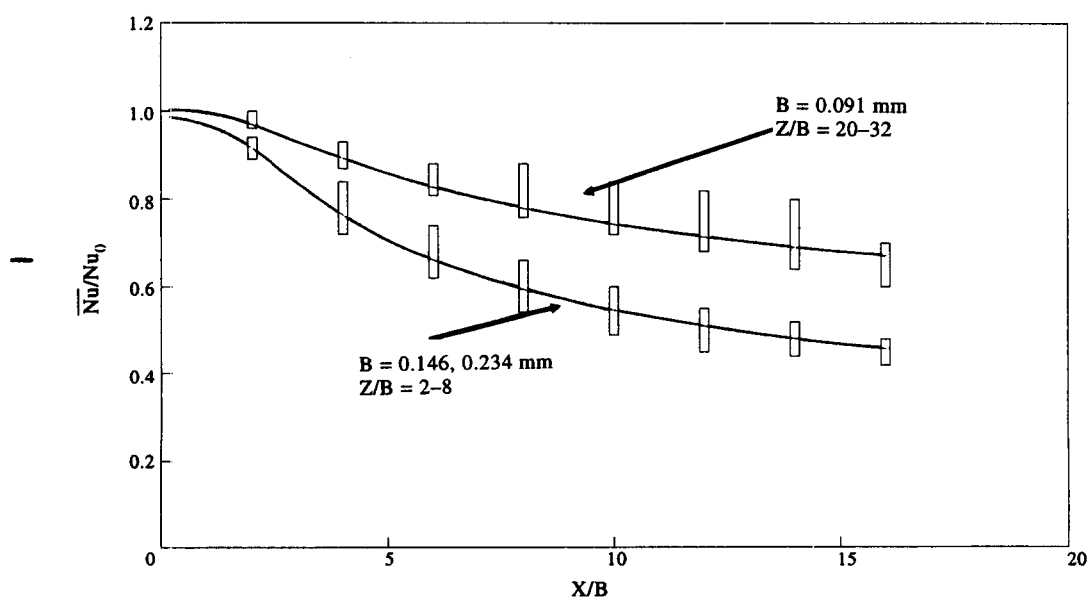

Fig. 12. Correlation of local average Nusselt number.

Table 3. Empirical constants in equation (12) and the correlation errors

Nozzle width [mm]	Z/B	$\bar{a}$	$\bar{b}$	$\bar{c}$	$\bar{d}$	$\bar{e}$	Average error	Standard deviation
0.091	20–32	0.5	0.05	1.255	−0.226	−11	±3.46%	5.27%
0.146	2–8	0.829	−1.027	1.302	−0.377	−13	±2.09%	3.16%
0.234	2–8	0.829	−1.027	1.302	−0.377	−13	±2.09%	3.16%

jets of transformer oil in the range of $Re = 55$–415. The nozzle width was from 0.091 mm to 0.234 mm. The jet exit velocity was between 4.86 and 13.53 m s^{-1}.

(2) Lateral variation of local recovery factor was determined at different Reynolds numbers and nozzle-to-plate spacings. Two symmetrical peaks were recorded near the stagnation line. The experimental data were found to agree well with the numerical result.

(3) Stagnation point heat transfer rates with the plate within the potential core can be well correlated by equation (7) for the nozzles of different widths. The effect of nozzle-to-plate spacing can be evaluated by equation (8).

(4) Bell-shaped lateral distribution of heat transfer coefficient can be correlated by equations (11) and (12) for local and average values respectively. Non-monotonic variations of Nusselt number with lateral distance and Reynolds number were recorded in wall jet zone, and ascribed to possible transition from laminar to turbulent regime.

Acknowledgements—This work was supported by the National Natural Science Foundation of China. The assistance of D. H. Lei and Y. P. Gan at Beijing Polytechnic University is appreciated. The authors also acknowledge the valuable suggestions of S. Y. Ko at Chinese Academy of Sciences, and F. Wang at Beijing University of Aeronautics.

REFERENCES

1. B. W. Webb and C. F. Ma, Single-phase liquid jet impingement heat transfer, *Adv. Heat Transfer* **26,** 105–217 (1995).
2. S. Inada, Y. Miyasaka and R. Izumi, A study on the laminar-flow heat transfer between a two-dimensional water jet and a flat surface with constant heat flux, *Bull. JSME* **24,** 1803–1810 (1981).
3. D. C. McMurray, P. S. Meyers and O. A. Uyehara, Influence of impinging jet variables on local heat transfer coefficients along a flat surface with constant heat flux, *Proceedings of the* 3 *International Heat Transfer Conference*, Vol, 2, pp. 292–299 (1966).
4. Y. Miyasaka and S. Inada, the effect of pure forced convection on the boiling heat transfer between a two-dimensional subcooled water jet and a heated surface, *J. Chem. Engng Jpn* **13,** 22–28 (1980).
5. D. T. Vader, F. P. Incropera and R. Viskanta, Local convective heat transfer from a heated surface to an impinging, planar jet of water, *Int. J. Heat Mass Transfer* **34,** 611–623 (1991).
6. D. T. Vader, F. P. Incropera and R. Viskanta, A method for measuring steady local heat transfer to an impinging liquid jet, *Exp. Therm. Fluid Sci.* **4,** 1–11 (1991).
7. D. H. Wolf, R. Viskanta and F. P. Incropera, Local convective heat transfer from a heated surface to a planar jet of water with a nonuniform velocity profile, *ASME J. Heat Transfer* **112,** 889–905 (1990).
8. D. H. Wolf, R. Viskanta and F. P. Incropera, Turbulence dissipation in a free-surface jet of water and its effect on local impingement heat transfer from a heated surface—II. Local heat transfer, *ASME J. Heat Transfer* **117,** 95–103 (1995).
9. D. A. Zumbrunnen, F. P. Incropera and R. Viskanta, Convective heat transfer distributions on a plate cooled by planar water jets, *ASME J. Heat Transfer* **111,** 899–896 (1989).
10. D. Schafer, F. P. Incropera and S. Ramadhyani, Planar liquid jet impingement cooling of multiple discrete heat sources, *ASME J. Electron. Packag.* **113,** 359–366 (1991).
11. C. B. Gu, G. S. Su, L. C. Chow and J. E. Beam, Heat transfer in two-dimensional jet impingement of a dielectric liquid on a plate with uniform heat flux, SAE Paper No. 921943 (1992).
12. D. C. Wadsworth and I. Mudawar, Cooling of a multichip electronic module by means of confined two-dimensional jets of dielectric liquid, *ASME J. Heat Transfer* **112,** 891–898 (1990).
13. H. Martin, Heat and mass transfer between impinging gas jets and solid surfaces, *Adv. Heat Transfer* **13,** 1–60 (1977).
14. M. N. Ozsik, *Heat Transfer, A Basic Approach*, pp. 296–297. McGraw-Hill, New York.
15. R. Gardon, and J. C. Akfirat, Heat transfer characteristics of impinging two-dimensional air jet, *ASME J. Heat Transfer*, **118,** 101–108 (1996).
16. B. Elison and B. W. Webb, Local heat transfer to impinging liquid jets in the initially laminar, transitional, and turbulent regimes, *Int. J. Heat Mass Transfer* **37,** 1207–1216 (1994).
17. M. Chen, Local heat transfer and laminar-turbulent transition with impinging submerged and free-surface slot jets of dielectric liquid, M.Sc. Thesis, Beijing Polytechnic University (1996).
18. E. M. Sparrow and T. C. Wong, Impingement transfer coefficients due to initially laminar slot jets, *Int. J. Heat Mass Transfer* **18,** 597–605 (1975).
19. C. F. Ma, H. Sun, H. Auracher and T. Gomi, Local convective heat transfer from vertical heated surfaces to impinging circular jets of large Prandtl number fluid, *Proceedings of the International Heat Transfer Conference*, Vol. 2, pp. 441–446 (1990).
20. H. Sun, C. F. Ma and W. Nakayama, Local characteristics of convective heat transfer from simulated microelectronic chips to impinging submerged round water jets, *J. Electron. Packag.* **115,** 71–77 (1993).
21. R. Gardon, and J. C. Akfirat, The role of turbulence in determining the heat-transfer characteristics of impinging jets, *Int. J. Heat Mass Transfer* **18,** 1261–1272 (1965).